

## Theory of helium adsorption on simple and noble-metal surfaces\*

E. Zaremba<sup>†</sup> and W. Kohn

*Department of Physics, University of California San Diego, La Jolla, California 92093*

(Received 20 July 1976)

The repulsive part of the helium-metal physisorption potential is calculated in the Hartree-Fock approximation. To the lowest order in the overlap ( $S$ ) between the atomic and metallic wave functions, this interaction is determined by the change in the single-particle density of states of the metal. Combined with a previous calculation of the Van der Waals interaction, helium-metal potentials are derived for the simple and noble metals using a jellium model for the metal. Binding energies and equilibrium positions of the helium atom are determined. For the simple metals, the binding energy decreases with increasing  $r_s$ . Its value for the noble metals is between 40 and 70 K. The equilibrium positions are found to be between 3 and 7 Å (relative to the jellium background) for all the metals studied.

### I. INTRODUCTION

The adsorption of rare-gas atoms on metallic surfaces is an example of physisorption. For these chemically inert adsorbates, the general features of the metal-atom interaction have been understood by analogy with the theory of rare-gas atom-atom interactions.<sup>1,2</sup> The total potential energy can be approximated as a sum of two parts—the attractive long-range Van der Waals<sup>3,4</sup> (or polarization) potential and a short-range repulsive potential associated with the overlap of the electrons of the adatom with those of the metal. Since the metal-atom attraction is due mainly to the weak Van der Waals force, the binding energy is relatively small ( $E_B \lesssim 0.5$  eV).

In a recent paper<sup>5</sup> we have derived an expression for the Van der Waals potential which is suitable in the problem of physisorption. The present paper is primarily devoted to the repulsive part of the metal-atom interaction. In calculating the repulsive potential, it is of course important to explicitly account for electronic exchange between the atom and metal. The simplest theory which includes these effects is the Hartree-Fock approximation; the repulsive potential is therefore defined in terms of the Hartree-Fock interaction (Sec. II).

It is found that the overlap of the unperturbed metallic density with the electronic density of the adatom is a convenient expansion parameter. For helium adsorption it is sufficient to treat the problem to first order in this parameter, since the He atom is located far from the metal surface. To this order, a number of simplifications can be made which allow a quantitative determination of the He-metal potential. The importance of higher-order terms for the other rare-gas atoms makes a similar theory for these atoms considerably more difficult. For this reason, we restrict ourselves to the theory of He physisorption.

To lowest order in the overlap, it is found that the Hartree-Fock interaction can be reduced to the calculation of the single-particle density of states for a system of electrons whose motion is determined by the effective potential due to the metal and the Hartree-Fock potential due to the bound He electrons. The change in the density of states which results from the He-metal overlap is calculated for a jellium model of the metal (Sec. III). This model incorporates the essential characteristics of the metal (valence electron density and work function) which are pertinent to an accurate estimate of the overlap. The results of Sec. III are then used to define He-metal potentials for the simple and noble metals (Sec. IV). The use of a jellium model for the latter metals is again justified on the basis of the large metal-atom equilibrium separations; at these separations, the valence-electron density produces the main contribution to the repulsion. Furthermore, recent studies<sup>6</sup> of Xe absorption on Ag indicate that even for the smaller metal-atom separations in this system, the close-packed surfaces are remarkably smooth, justifying the use of a model which is translationally invariant along the surface.

The calculated He-metal potentials are used to determine various characteristics (e.g., binding energy, equilibrium position, etc.) of the adsorbed atom. Trends in these quantities as a function of the metallic density,  $\bar{n} = (\frac{4}{3}\pi r_s^3)^{-1}$ , are found to differ notably from the results of Kleiman and Landman.<sup>7</sup> The differences stem partly from their incomplete definition of the repulsive interaction; these aspects are discussed in more detail in Secs. III and IV.

The conventional division of the full physisorption interaction into an attractive and repulsive part, which we follow in the present paper, is of course not strict. However, in the particular case of the He-metal system, we believe that be-

cause of the small polarizability of the atom, the present treatment gives a good account of the physisorption potential.

## II. METAL-ATOM INTERACTION

### A. General considerations

We are considering the situation depicted in Fig. 1 of an atom located at a position  $Z$  relative to a metallic surface. Quite generally, the potential energy of the atom is defined as the change in the ground-state energy of the system that occurs as the atom is brought in from infinity, i.e.,

$$V(Z) = E(Z) - E(\infty) \\ = \langle \Psi_Z | H | \Psi_Z \rangle - \langle \Psi_\infty | H | \Psi_\infty \rangle. \quad (2.1)$$

Here,  $|\Psi_Z\rangle$  is the many-body electronic wave function for the metal-atom system with separation  $Z$ . The Hamiltonian  $H$  consists of three pieces,

$$H = H_a + H_m + H_{am}, \quad (2.2)$$

where  $H_a$  and  $H_m$  are, respectively, the Hamiltonians for the isolated atomic and metallic systems, and  $H_{am}$  is the mutual interaction between these two subsystems. Explicitly, this Hamiltonian includes kinetic-energy terms plus the Coulomb interactions between all the charges in the system.

In the following, it is convenient to separate  $V(Z)$  into the Hartree-Fock (HF) result  $V_{\text{HF}}(Z)$  and a remainder which is conventionally referred to as the correlation contribution:

$$V(Z) = V_{\text{HF}}(Z) + V_{\text{corr}}(Z). \quad (2.3)$$

The HF contribution is obtained using an antisymmetrized product of single-particle wave functions which are solutions of the usual HF equations. For the case of He on a simple metal, one of the states lies below the band of metallic states<sup>9</sup> (see Fig. 1) and corresponds to the core

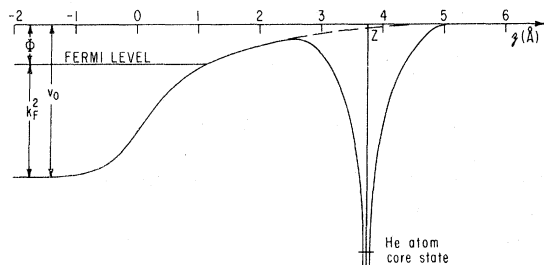


FIG. 1. Schematic illustration of the nonlocal helium-atom potential near the surface of a metal. As drawn, the metallic potential is representative of aluminum. The position of the atomic potential is at the calculated equilibrium position of a He atom on an aluminum surface. The origin is chosen at the edge of the positive background.

state of the He atom. The remaining wave functions describe propagating metallic states which are perturbed in the vicinity of the atom.

Because of the localization of these wave functions in the respective subsystems,  $V_{\text{HF}}(Z)$  is an exponentially decreasing function of  $Z$  and for sufficiently large separations,  $V_{\text{corr}}(Z)$  dominates. This latter contribution is just the Van der Waals interaction between the atom and the metal and can be calculated by perturbation theory. Since the overlap between the atomic and metallic wave functions is negligible in this region, the antisymmetry requirement for the interchange of electrons between the two subsystems need not be imposed. This interaction has been obtained previously<sup>3-5</sup> and takes the form

$$V_{\text{corr}} = -C/(Z - Z_0)^3. \quad (2.4)$$

The constant  $C$  is a measure of the strength of the Van der Waals interaction and  $Z_0$  defines a reference plane with respect to which the position of the atom is to be determined. Values of  $C$  and  $Z_0$  for the He-jellium system are given in Ref. 5.

At intermediate and small separations corrections to the asymptotic form of the correlation energy (2.4) will occur due to electron overlap. However, since the equilibrium position of the He atom is in a region where the metallic density is small (see Sec. IV), it is reasonable to expect the asymptotic form to be a good approximation. In using this result, one is neglecting those correlation effects related to a metallic electron being found near the atom. Owing to the rigidity of the He ground-state wave function, these corrections are probably small.

Our basic assumption therefore is that the potential energy can be determined from (2.3) with the correlation contribution given by (2.4). Although this procedure is not rigorously justified, it has frequently been used in discussions of molecular interactions<sup>9</sup> and should work equally well for the helium adsorption problem. In any case, the quantities considered and evaluated here would still be required in a more complete theory which includes those modifications to the correlation energy arising from the wave-function overlap.

### B. Hartree-Fock interaction

In the Hartree-Fock approximation, the wave function is given by the antisymmetrized product

$$\Psi = A \prod_i \psi_{\alpha_i}(\vec{r}_i), \quad (2.5)$$

and the corresponding ground-state energy is

$$E_{\text{HF}} = 2 \sum_{\lambda} e_{\lambda} - \sum_{\lambda\mu} (2 \langle \lambda\mu | v | \lambda\mu \rangle - \langle \lambda\mu | v | \mu\lambda \rangle). \quad (2.6)$$

Here the electronic spin degeneracy is accounted for explicitly and the index  $\lambda$  refers to the orbital part of the single-particle wave functions;  $\epsilon_\lambda$  are the energy eigenvalues of the HF equations; and the remaining terms are the direct and exchange matrix elements of the Coulomb potential.

For the problem we are considering, the single-particle wave functions  $\psi_\lambda(\vec{r})$  satisfy the HF equations (atomic units)

$$\left( -\frac{1}{2} \nabla^2 - \frac{2}{r} + v_+(\vec{r}) + 2 \int d\vec{r}' \sum_\mu \frac{|\psi_\mu(\vec{r}')|^2}{|\vec{r} - \vec{r}'|} \right) \psi_\lambda(\vec{r}) - \int d\vec{r}' \sum_\mu \frac{\psi_\mu(\vec{r}) \psi_\mu^*(\vec{r}') \psi_\lambda(\vec{r}')}{|\vec{r} - \vec{r}'|} = \epsilon_\lambda \psi_\lambda(\vec{r}). \quad (2.7)$$

The terms  $(-2/r)$  and  $v_+(\vec{r})$ , respectively, represent the potentials of the He nucleus and the positive metallic background.

On subtracting the HF energy for the separated systems, we obtain

$$V_{\text{HF}}(Z) = 2 \sum_i \delta \epsilon_i + 2 \delta \epsilon_a - \delta \sum_{ij} (2 \langle ij | v | ij \rangle - \langle ij | v | ji \rangle) - \langle aa | v | aa \rangle - 2 \sum_i (2 \langle ia | v | ia \rangle - \langle ia | v | ai \rangle) + \langle a_0 a_0 | v | a_0 a_0 \rangle - 2v_+(R_a). \quad (2.8)$$

Here we have distinguished between the atomic ( $a$ ) and metallic states ( $i, j$ ).  $R_a$  is the position of the adatom nucleus. The first two terms in (2.8) give the change in the single-particle eigenvalues; the next term is the change in the Coulomb energy of the metallic electrons; and the last term is the electrostatic interaction between the He nucleus and the positive background. The HF wave function for the isolated He atom is denoted by  $\psi_a^0(\vec{r}) = \langle \vec{r} | a_0 \rangle$ .

Equation (2.8) can now be simplified by obtaining an expression for the shift in the atomic eigenvalue  $\epsilon_a$ . In terms of the unperturbed atomic HF Hamiltonian

$$H_0 \equiv -\frac{1}{2} \nabla^2 - \frac{2}{r} + \int d\vec{r}' \frac{|\psi_a^0(\vec{r}')|^2}{|\vec{r} - \vec{r}'|}, \quad (2.9)$$

the HF equation for the atomic state can be written as

$$(H_0 + \delta \hat{V}) \psi_a(\vec{r}) = \epsilon_a \psi_a(\vec{r}), \quad (2.10)$$

where  $\delta \hat{V}$  is a small perturbation of order the overlap between the atomic and metallic states. Specifically, a measure of this perturbation is given by the parameter

$$S \equiv \int d\vec{r} n_0(\vec{r}) |\psi_a^0(\vec{r})|^2, \quad (2.11)$$

where  $n_0(\vec{r})$  is the unperturbed metallic density. This overlap parameter is basically proportional

to  $(r_0/r_{s,loc})^3$ ,  $r_0$  being the atomic radius and  $r_{s,loc}$  the Wigner-Seitz radius corresponding to the average metallic density in the atomic region. For large separations,  $S$  is indeed small and is the appropriate expansion parameter to be used in the following.

Taking the matrix element of (2.10) with the atomic state  $\psi_a(\vec{r})$ , we obtain

$$\epsilon_a = \langle a | H_0 | a \rangle + \langle aa | v | aa \rangle - \langle aa_0 | v | aa_0 \rangle + \sum_i (2 \langle ia | v | ia \rangle - \langle ia | v | ai \rangle) + \langle a | v_+ | a \rangle. \quad (2.12)$$

Since the expectation value of  $H_0$  is stationary about the unperturbed atomic state, we have

$$\langle a | H_0 | a \rangle = \langle a_0 | H_0 | a_0 \rangle + O((\delta \psi_a)^2) = \epsilon_a^0 + O((\delta \psi_a)^2), \quad (2.13)$$

where  $\delta \psi_a(\vec{r}) \equiv \psi_a(\vec{r}) - \psi_a^0(\vec{r})$  is the change in the atomic state. As stated previously,  $\delta \psi_a$  is of order  $S$ , the overlap. Thus, to first order in  $S$ , the first term in (2.12) can be replaced by  $\epsilon_a^0$ .

Using (2.12) and (2.13) in (2.8), we find

$$V_{\text{HF}}(Z) = 2 \sum_i \delta \epsilon_i - \delta \sum_{ij} (2 \langle ij | v | ij \rangle - \langle ij | v | ji \rangle) + \langle aa | v | aa \rangle + \langle a_0 a_0 | v | a_0 a_0 \rangle - 2 \langle aa_0 | v | aa_0 \rangle + 2 \langle a | v_+ | a \rangle - 2v_+(R_a). \quad (2.14)$$

The atomic matrix elements of the Coulomb potential cancel to order  $S$ . In addition, a similar consideration of the HF equations for the metallic states reveals that the last two terms in (2.14) are in fact cancelled to  $O(S^2)$ . Thus, (2.14) finally reduces to

$$V_{\text{HF}}(Z) = 2 \sum_i \delta \epsilon_i - \delta \sum_{ij} (2 \langle ij | v | ij \rangle - \langle ij | v | ji \rangle) + O(S^2). \quad (2.15)$$

To lowest order in  $S$ , the atomic state does not appear explicitly in the HF interaction. To the same order, the metallic states  $\psi_i(\vec{r})$  are determined by (2.7) with  $\psi_a(\vec{r})$  replaced by  $\psi_a^0(\vec{r})$ . Thus, to this order,  $V_{\text{HF}}(Z)$  is simply determined by the change in the HF energy of the metallic electrons induced by the nonlocal HF potential of the He atom.

The solution of (2.7) for the metallic states remains a formidable problem in view of the apparent requirement of self-consistency. However, since the main perturbation is the presence of the atomic potential, the requirement for self-consistency is actually of secondary importance. In particular, it is sufficient to evaluate (2.15) using the solutions of the following equation

$$\left(-\frac{1}{2}\nabla^2 - \frac{2}{r} + v_+(\vec{r}) + 2 \int d\vec{r}' \sum_{\lambda} \frac{|\psi_{\lambda}^0(\vec{r}')|^2}{|\vec{r}-\vec{r}'|}\right)\tilde{\psi}_i(\vec{r}) - \int d\vec{r}' \sum_{\lambda} \frac{\psi_{\lambda}^0(\vec{r})\psi_{\lambda}^{0*}(\vec{r}')\tilde{\psi}_i(\vec{r}')}{|\vec{r}-\vec{r}'|} = \tilde{\epsilon}_i \tilde{\psi}_i(\vec{r}). \quad (2.16)$$

If the metallic density generated by  $\tilde{\psi}_i(\vec{r})$  is denoted by  $\tilde{n}(\vec{r})$ , the difference between  $n(\vec{r})$ , the correct self-consistent density, and  $\tilde{n}(\vec{r})$  is everywhere small and of the order of the overlap,  $S$ . Thus, due to the stationary property of the metallic HF energy, evaluating (2.15) using the solutions to (2.16) introduces an error of the order ( $S^2$ ).

The HF energy using the solutions of (2.16) is

$$\begin{aligned} \tilde{E}_{\text{HF}} &= 2 \sum_i \delta\tilde{\epsilon}_i + \sum_{ij} 2(\langle ij | v | ij \rangle - 2\langle ij_0 | v | ij_0 \rangle) \\ &- \sum_{ij} (\langle ij | v | ji \rangle - 2\langle ij_0 | v | j_0 i_0 \rangle). \end{aligned} \quad (2.17)$$

Here,  $\langle \vec{r} | i \rangle$  denotes  $\tilde{\psi}_i(\vec{r})$  and  $|i_0\rangle$  is the unperturbed metallic state. We now subtract  $E_{\text{HF}}^0$  from (2.17) and expand  $|i\rangle$  as  $|i\rangle \equiv |i_0\rangle + |i_1\rangle$ . Carrying out this expansion, we find

$$\begin{aligned} V_{\text{HF}}(Z) &\approx 2 \sum_i \delta\tilde{\epsilon}_i \\ &+ 2 \sum_{ij} (2\langle i_1 j_1 | v | i_0 j_0 \rangle - \langle i_1 j_1 | v | j_0 i_0 \rangle) \\ &+ \dots, \end{aligned} \quad (2.18)$$

where the dots represent higher-order terms in  $|i_1\rangle$ . Since the product  $\psi_i^0(\vec{r})\delta\psi_i^*(\vec{r})$  is at least of order  $S$ , the matrix elements in (2.18) are of  $O(S^2)$  and can be neglected. Thus, to lowest order,  $V_{\text{HF}}(Z)$  can be approximated as the sum over the eigenvalue shifts. In effect, the Coulomb interactions can be neglected and the interaction energy is the same as would be obtained for a system of noninteracting electrons.

The sum of the eigenvalue shifts is determined most conveniently in terms of the change in the metallic density of states  $\Delta\rho(\epsilon)$ . Once  $\Delta\rho(\epsilon)$  is found,  $V_{\text{HF}}(Z)$  is given by

$$V_{\text{HF}}(Z) = \int_0^{\epsilon_F} d\epsilon (\epsilon - \epsilon_F) \Delta\rho(\epsilon), \quad (2.19)$$

where  $\epsilon_F$  is the Fermi energy.

In Sec. III we take up the problem of determining  $\Delta\rho(\epsilon)$ . In doing so, we simplify (2.16) by replacing the unperturbed HF potential for the metal by a local effective potential  $v_m(\vec{r})$ . Our actual numerical results are based on the Lang-Kohn<sup>10</sup> self-consistent potentials for  $v_m(\vec{r})$ . Since these latter potentials include correlation effects they are not equivalent to the HF potential required in (2.16). However, since  $\Delta\rho(\epsilon)$  is sensitive to the metallic

density far from the surface, it is important that this density be accurately reproduced. For this purpose, the Lang-Kohn potentials are the most satisfactory which are available. In a certain sense, their use can be thought of as going beyond the simple HF theory to the extent that an accurate representation of the metallic density is used.

It is of interest to compare our result given in (2.19) with the recent work of Kleiman and Landman.<sup>7</sup> These authors consider the repulsive energy as due to the change in the kinetic energy which results when the atom overlaps with the metallic density. Using the density functional formalism, they evaluate this energy by making a local approximation to the kinetic-energy functional. Further, they assume the metallic density to be unchanged from its free metal form. This procedure is inadequate for a number of reasons. Most importantly, the interaction energy is not simply the change in kinetic energy but is in fact more closely related to the shift in eigenvalues as either a noninteracting electron gas model or our explicit derivation in the HF approximation shows. In neglecting the energy associated with the metallic electrons interacting with the atomic potential, they have overestimated the repulsive contribution. Secondly, the use of the unperturbed metallic density in the vicinity of the atom is a poor approximation, as demonstrated in Fig. 6, and so their estimated values for the change in the kinetic energy are unreliable.

### III. CHANGE IN THE SINGLE-PARTICLE DENSITY OF STATES

The problem of obtaining  $\Delta\rho(\epsilon)$  as posed in the previous section is analogous to the usual Friedel impurity problem, although complicated somewhat by the reduced symmetry in the adsorption geometry. Nonetheless, a formal result due to Langer and Ambegaokar<sup>11</sup> can be used which gives  $\Delta\rho(\epsilon)$  in terms of the  $\mathcal{S}$  matrix,<sup>12</sup>

$$\Delta\rho(\epsilon) = \frac{1}{2\pi i} \text{Tr} \frac{\partial}{\partial \epsilon} \ln \mathcal{S}(\epsilon). \quad (3.1)$$

The  $\mathcal{S}$  operator is defined in terms of the  $\mathcal{T}$  matrix

$$\mathcal{S}(\epsilon) = 1 - 2\pi i \delta(\epsilon - H^0) \mathcal{T}(\epsilon + i\delta), \quad (3.2)$$

where

$$\mathcal{T}(\epsilon + i\delta) = V[1 - G^0(\epsilon + i\delta)V]^{-1}. \quad (3.3)$$

$G^0(\epsilon + i\delta) = (\epsilon + i\delta - H^0)^{-1}$  is the Green's function for the unperturbed metal;  $H^0$  is the metal Hamiltonian; and  $V$  is the potential of the adatom which here represents the impurity. The trace operation in (3.1) is taken over a complete set of states,  $|\epsilon'\lambda\rangle$ . Owing to the structure of (3.1), the trace

can be restricted to those states  $|\epsilon\lambda\rangle$  having the energy  $\epsilon$ ,<sup>12</sup>

$$\Delta\rho(\epsilon) = \frac{1}{2\pi i} \frac{\partial}{\partial\epsilon} \text{Tr}_{(\lambda)} \ln[1 - 2\pi i T(\epsilon + i\delta)] \quad (3.4)$$

where  $T(\epsilon + i\delta)$  is the on-shell  $T$  matrix,

$$\langle\lambda|T(\epsilon + i\delta)|\lambda'\rangle \equiv \langle\epsilon\lambda|T(\epsilon + i\delta)|\epsilon\lambda'\rangle. \quad (3.5)$$

When the adatom sits far from the surface, the matrix elements of  $T$  are small, being of the order of the overlap. The logarithm in (3.4) can therefore be expanded in powers of  $T$ . Retaining only the lowest-order term,

$$\Delta\rho(\epsilon) = -\frac{\partial}{\partial\epsilon} \text{Tr}_{(\lambda)} T(\epsilon + i\delta) + O(S^2). \quad (3.6)$$

It should be emphasized that this is an expansion in  $S$ , and is not equivalent to an expansion in the impurity potential  $V$ , which is a strong perturbation.

In the form given in (3.6), we require only the (diagonal) matrix elements of  $T$ . These matrix elements are related to those of  $V$  by<sup>13</sup>

$$T_{\lambda,\lambda}(\epsilon) \equiv \langle\lambda'|T(\epsilon + i\delta)|\lambda\rangle = \langle\epsilon\lambda'|V|\epsilon\lambda\rangle, \quad (3.7)$$

where  $|\epsilon\lambda\rangle$  is a scattering state satisfying the Lippmann-Schwinger equation

$$|\epsilon\lambda\rangle = |\epsilon\lambda\rangle + G^0(\epsilon + i\delta)V|\epsilon\lambda\rangle. \quad (3.8)$$

In coordinate representation, this equation becomes

$$\psi_{\epsilon\lambda}^{(+)}(\vec{r}) = \psi_{\epsilon\lambda}^0(\vec{r}) + \int d\vec{r}' G^0(\vec{r}, \vec{r}', \epsilon + i\delta) V(\vec{r}') \psi_{\epsilon\lambda}^{(+)}(\vec{r}'). \quad (3.9)$$

$\psi_{\epsilon\lambda}^0(\vec{r})$  is an eigenfunction of  $H^0$ . We have here indicated that  $V$  is a local operator although the following development does not depend on this assumption. The evaluation of (3.7) is thus reduced to finding the solution to (3.9).

This solution is obtained by noting that equation (3.9) is equivalent to the Schrödinger equation

$$[\epsilon - H^0 - V(r)] \psi_{\epsilon\lambda}^{(+)}(\vec{r}) = 0. \quad (3.10)$$

Assuming  $V(r)$  to have a finite range,  $r_0$ , the integral in (3.9) is restricted to  $|\vec{r}'| \leq r_0$ . Substituting  $V(r)\psi_{\epsilon\lambda}^{(+)}(\vec{r})$  from (3.10) into (3.9) and

making use of Green's theorem, we obtain

$$\psi_{\epsilon\lambda}^0(\vec{r}) + \int_S dS' \left( G^0(\vec{r}, \vec{r}', \epsilon) \frac{\partial \psi_{\epsilon\lambda}^{(+)}(\vec{r}')}{\partial n'} - \frac{\partial G^0(\vec{r}, \vec{r}', \epsilon)}{\partial n'} \psi_{\epsilon\lambda}^{(+)}(\vec{r}') \right) = 0 \quad (3.11)$$

with  $|\vec{r}| < r_0$ . Here the integral is taken over the surface of a sphere of radius  $r_0$  surrounding the adatom;  $\partial/\partial n$  represents an outward normal derivative. Similarly, (3.7) can be written as

$$T_{\lambda,\lambda}(\epsilon) = \int_S dS \left( \psi_{\epsilon\lambda}^{0*}(\vec{r}) \frac{\partial \psi_{\epsilon\lambda}^{(+)}(\vec{r})}{\partial n} - \frac{\partial \psi_{\epsilon\lambda}^{0*}(\vec{r})}{\partial n} \psi_{\epsilon\lambda}^{(+)}(\vec{r}) \right). \quad (3.12)$$

The integral equation in (3.11) is now reduced to a system of linear equations by expanding  $\psi_{\epsilon\lambda}^0(r)$  and  $\psi_{\epsilon\lambda}^{(+)}(r)$  for  $|r| < r_0$  in spherical harmonics:

$$\psi_{\epsilon\lambda}^{(+)}(\vec{r}) = \sum_{l,m} a_{lm}(\epsilon\lambda) R_l(r, \epsilon) Y_{lm}(\Omega) \quad (3.13a)$$

and

$$\psi_{\epsilon\lambda}^0(r) = \sum_{l,m} b_{lm}(\epsilon\lambda, r) Y_{lm}(\Omega). \quad (3.13b)$$

The function  $R_l(r, \epsilon)$  is the solution of the radial Schrödinger equation (Rydberg units)

$$\left[ -\frac{1}{r^2} \frac{d}{dr} \left( r^2 \frac{d}{dr} \right) + \frac{l(l+1)}{r^2} + V(r) \right] R_l(r, \epsilon) = \epsilon R_l(r, \epsilon) \quad (3.14)$$

which satisfies  $R_l(r_0, \epsilon) = 1$ . The expansion coefficients  $b_{lm}(\epsilon\lambda, r)$  are given by

$$b_{lm}(\epsilon\lambda, r) \equiv \int d\Omega Y_{lm}^*(\Omega) \psi_{\epsilon\lambda}^0(\vec{r}). \quad (3.15)$$

Using these expansions in (3.11) and taking the limit  $|\vec{r}| \rightarrow r_0$ , we obtain the inhomogeneous system of linear equations

$$r_0^2 \sum_{l',m'} [G'_{lm,l'm'}(\epsilon) - L_{l'}(\epsilon) G_{lm,l'm'}(\epsilon)] a_{l'm'}(\epsilon\lambda) = b_{lm}(\epsilon\lambda, r_0). \quad (3.16)$$

Here we have defined

$$G_{lm,l'm'}(\epsilon) = \lim_{\eta \rightarrow 0} \int d\Omega \int d\Omega' Y_{lm}^*(\Omega) G^0(r_0 - \eta, \Omega, r_0, \Omega', \epsilon) Y_{l'm'}(\Omega'), \quad (3.17a)$$

$$G'_{lm,l'm'}(\epsilon) = \lim_{\eta \rightarrow 0} \int d\Omega \int d\Omega' Y_{lm}^*(\Omega) \frac{d}{dr'} G^0(r_0 - \eta, \Omega, r', \Omega', \epsilon) \Big|_{r'=r_0} Y_{l'm'}(\Omega'), \quad (3.17b)$$

and the logarithmic derivative

$$L_l(\epsilon) = R'_l(r_0, \epsilon) / R_l(r_0, \epsilon). \quad (3.18)$$

Similarly, (3.12) reduces to

$$T_{\lambda\lambda'}(\epsilon) = r_0^2 \sum_{l,m} \left( b_{lm}^*(\epsilon\lambda, r_0) L_l(\epsilon) - \frac{d}{dr_0} b_{lm}^*(\epsilon\lambda, r_0) \right) a_{lm}(\epsilon\lambda'). \quad (3.19)$$

In order to explicitly evaluate  $T_{\lambda\lambda'}(\epsilon)$  we therefore require: (i) the free-metal Green's function  $G^0(\vec{r}, \vec{r}', \epsilon)$  and the matrix elements  $G_{lm, l'm'}$  and  $G'_{lm, l'm'}$ ; (ii) the unperturbed metal eigenfunctions  $\psi_{\epsilon\lambda}^0(\vec{r})$  and the expansion coefficients  $b_{lm}(\epsilon\lambda, r_0)$ ; (iii) the logarithmic derivatives,  $L_l(\epsilon)$ ; and (iv) the coefficients  $a_{lm}(\epsilon\lambda)$  as obtained from (3.16). These various aspects are discussed in the following.

#### A. Free-metal Green's function

The Green's function appearing in (3.9) is the causal (or outgoing) solution of

$$[\nabla^2 + \epsilon - v_m(\vec{r})] G^0(\vec{r}, \vec{r}', \epsilon) = \delta(\vec{r} - \vec{r}'). \quad (3.20)$$

The metallic potential  $v_m(\vec{r})$  is assumed to be a function of  $z$  only and is indicated schematically in Fig. 1. Because of the translational invariance along the surface, we take the Fourier transform of  $G^0(\vec{r}, \vec{r}', \epsilon)$  with respect to the variable  $(\vec{p} - \vec{p}')$ :

$$G^0(z, z', \epsilon, q) = \int d(\vec{p} - \vec{p}') e^{i\vec{q} \cdot (\vec{p} - \vec{p}')} G^0(\vec{r}, \vec{r}', \epsilon) [\vec{r} = (\vec{p}, z)], \quad (3.21a)$$

$$G^0(\vec{r}, \vec{r}', \epsilon) = \int \frac{d\vec{q}}{(2\pi)^2} e^{-i\vec{q} \cdot (\vec{p} - \vec{p}')} G^0(z, z', \epsilon, q). \quad (3.21b)$$

$G^0(z, z', \epsilon, q)$  is the solution of the following differential equation:

$$\left( \frac{d^2}{dz^2} + \epsilon - q^2 - v_m(z) \right) G^0(z, z', \epsilon, q) = \delta(z - z'). \quad (3.22)$$

We are of course interested in solutions to (3.22) for energies  $\epsilon$  less than the barrier height,  $v_0$ . Since  $q^2$  ranges between 0 and  $\infty$ , there are two cases to consider depending upon whether  $\epsilon - q^2$  is greater than or less than zero.

Case (i):  $\epsilon - q^2 < 0$

In this case we have exponentially decaying solutions everywhere. Using standard techniques,<sup>14</sup> the solution to (3.22) can be obtained in terms of two linearly independent solutions of the homo-

geneous equation:

$$\left( \frac{d^2}{dz^2} - \kappa^2 - v_m(z) \right) g_{1,2}(z) = 0; \quad \kappa^2 = q^2 - \epsilon > 0. \quad (3.23)$$

The two solutions of (3.23) are chosen to have the following asymptotic behavior

$$g_1(z) \underset{z \rightarrow +\infty}{\sim} e^{-\beta z}, \quad \beta^2 = \kappa^2 + v_0 \quad (3.24a)$$

and

$$g_2(z) \underset{z \rightarrow -\infty}{\sim} e^{+\kappa z}. \quad (3.24b)$$

In terms of these solutions, the Green's function is given by

$$G^0(z, z', \epsilon, q) = \begin{cases} -g_1(z)g_2(z')/W[g_1, g_2], & z > z' \\ -g_1(z')g_2(z)/W[g_1, g_2], & z < z' \end{cases} \quad (3.25)$$

where  $W[g_1, g_2] \equiv g_1 g_2' - g_1' g_2$  is the Wronskian. In this energy range, the Green's function is real.

Owing to the particular geometry we are considering, we are interested in the case when  $z$  and  $z'$  are both large ( $z, z' \rightarrow +\infty$ ). In this region,  $g_2(z)$  behaves as

$$g_2(z) \sim a e^{-\beta z} + b e^{\beta z}, \quad (3.26)$$

so that (3.25) simplifies to

$$G^0(z, z', \epsilon, q) \Big|_{(z, z') \rightarrow +\infty} \sim -\frac{a}{b} \frac{1}{2\beta} e^{-\beta(z+z')} - \frac{1}{2\beta} e^{-\beta|z-z'|}. \quad (3.27)$$

The constants  $a$  and  $b$  depend upon the details of the potential  $v_m(z)$ .

Case (ii):  $\epsilon - q^2 > 0$

Defining  $k^2 = \epsilon - q^2$ ,  $g_{1,2}(z)$  satisfy

$$\left( \frac{d^2}{dz^2} + k^2 - v_m(z) \right) g_{1,2}(z) = 0. \quad (3.28)$$

It is convenient to choose these solutions to have the asymptotic form

$$g_1(z) \sim a_1 e^{-\beta z} \quad \text{as } z \rightarrow +\infty, \quad (3.29a)$$

$$g_2(z) \sim a_2 e^{\beta z} \quad \text{as } z \rightarrow +\infty, \quad (3.29b)$$

where  $\beta^2 = v_0 - k^2$ . The normalization of these functions is chosen such that  $g_{1,2}(z)$  are sine waves of unit amplitude for  $z \rightarrow -\infty$ :

$$g_{1,2}(z) \sim \sin(kz + \eta_{1,2}). \quad (3.30)$$

The two phase shifts  $\eta_1$  and  $\eta_2$  are functions of  $k$ . Imposing the condition that  $G^0(z, z', \epsilon, q)$  represent an outgoing Green's function, we find

$$G^0(z, z', \epsilon, q) = \frac{1}{k \sin(\eta_1 - \eta_2)} \begin{cases} e^{i(\eta_2 - \eta_1)g_1(z)g_1(z')} - g_1(z)g_2(z') \\ e^{i(\eta_2 - \eta_1)g_1(z')g_1(z)} - g_1(z')g_2(z) \end{cases}, \quad z > z' \quad (3.31)$$

Again we are interested in the large  $(z, z')$  limit for which (3.31) reduces to

$$G^0(z, z', \epsilon, q) |_{(z, z') \rightarrow +\infty} \sim (1/k) [\cot(\eta_1 - \eta_2) - i] |a_1|^2 e^{-\beta(z+z')} - (1/2\beta) e^{-\beta|z-z'|}. \quad (3.32)$$

It can easily be verified that the imaginary part of this function is the same as obtained by using the usual spectral representation.

Combining the results in (3.25) and (3.31),  $G^0(\vec{r}, \vec{r}', \epsilon)$  can be represented generally as

$$G^0(\vec{r}, \vec{r}', \epsilon) = G_d(\vec{r}, \vec{r}', \epsilon) + G_r(\vec{r}, \vec{r}', \epsilon), \quad (3.33)$$

where the "direct" propagator has the behavior

$$G_d(\vec{r}, \vec{r}', \epsilon) \underset{(z, z') \rightarrow +\infty}{\sim} -e^{-\alpha|\vec{r}-\vec{r}'|}/4\pi |\vec{r}-\vec{r}'|; \quad \alpha^2 = v_0 - \epsilon. \quad (3.34)$$

This is just the free-space propagator at negative energies. The "reflection" term  $G_r(\vec{r}, \vec{r}', \epsilon)$  comes from that part of  $G^0(z, z', \epsilon, q)$  which behaves as  $e^{-\beta(z+z')}$  for large  $z$  and  $z'$ . Although a closed-form expression cannot be obtained for  $G_r(\vec{r}, \vec{r}', \epsilon)$ , it is clear that it is a much smaller term than  $G_d(\vec{r}, \vec{r}', \epsilon)$  in this region (in fact, it is of order  $S$  relative to  $G_d$ ). This property is clarified by referring to Fig. 2, where it is seen that the propagation along path (b) is much longer than along path (a). Since the particle is at negative energies in this region, the propagators along these paths are exponentially decreasing. Thus, if the adatom is sufficiently far from the surface, only  $G_d(\vec{r}, \vec{r}', \epsilon)$  need be considered.

Using the form given in (3.34) for  $G^0(\vec{r}, \vec{r}', \epsilon)$ , Eqs. (3.17) can be evaluated straightforwardly with the result

$$G_{lm, l'm'} \simeq \delta_{ll'} \delta_{mm'} \alpha j_l(i\alpha r_0) h_l^{(1)}(i\alpha r_0) \quad (3.35a)$$

and

$$G'_{lm, l'm'} \simeq \delta_{ll'} \delta_{mm'} i\alpha^2 j_l(i\alpha r_0) h_l^{(1)'}(i\alpha r_0), \quad (3.35b)$$

where  $j_l(x)$  and  $h_l^{(1)}(x)$ , respectively, are the spherical Bessel function and spherical Hankel function of the first kind.<sup>15</sup>

#### B. $b_{lm}(\epsilon\lambda, r_0)$

In evaluating  $b_{lm}(\epsilon\lambda, r_0)$  we have chosen the unperturbed wave functions to be

$$\psi_{\epsilon km}^0 \equiv (2\pi^2)^{-1/2} e^{im\phi} J_m(q\rho) u_k(z), \quad \epsilon = q^2 + k^2 \quad (3.36)$$

where  $J_m(x)$  is the cylindrical Bessel function of order  $m$ ,<sup>15</sup> and  $u_k(z)$  is that wave function denoted as  $g_1(z)$  in (3.28). These functions satisfy the orthogonality condition

$$\int d\vec{r} \psi_{\epsilon' k' m'}^0(\vec{r})^* \psi_{\epsilon km}^0(\vec{r}) = \delta_{mm'} \delta(\epsilon - \epsilon') \delta(k - k') \quad (3.37)$$

and the completeness relation

$$\sum_{m=-\infty}^{\infty} \int_0^{\infty} d\epsilon \int_0^{\epsilon^{1/2}} dk \psi_{\epsilon km}^0(\vec{r})^* \psi_{\epsilon km}^0(\vec{r}') = \delta(\vec{r} - \vec{r}'). \quad (3.38)$$

Using these functions,  $b_{lm}(\epsilon\lambda, r_0)$  and  $db_{lm}(\epsilon\lambda, r_0)/dr_0$  can be written as

$$b_{l\bar{m}}(\epsilon km, r_0) \equiv \delta_{m\bar{m}} b_l'(\epsilon km) \quad (3.39a)$$

and

$$\frac{db_{l\bar{m}}(\epsilon km, r_0)}{dr_0} \equiv \delta_{m\bar{m}} b_l''(\epsilon km). \quad (3.39b)$$

In the region in which  $u_k(z)$  behaves as shown in (3.29a), we find

$$b_l(\epsilon km) = e^{-\beta z} \left( \frac{2l+1}{2\pi} \frac{(l-m)!}{(l+m)!} \right)^{1/2} \int_{-1}^1 dx P_l^m(x) J_m(qr_0(1-x^2)^{1/2}) u_k(r_0 x) \quad (3.40a)$$

and

$$b_l'(\epsilon km) = e^{-\beta z} \left( \frac{2l+1}{2\pi} \frac{(l-m)!}{(l+m)!} \right)^{1/2} \int_{-1}^1 dx P_l^m(x) u_k(r_0 x) \\ \times \left\{ \frac{1}{2} q(1-x^2)^{1/2} [J_{m-1}(qr_0(1-x^2)^{1/2}) - J_{m+1}(qr_0(1-x^2)^{1/2})] \right. \\ \left. - \beta x J_m(qr_0(1-x^2)^{1/2}) \right\}. \quad (3.40b)$$

Here  $P_l^m(x)$  is the associated Legendre function<sup>15</sup> and  $Z$  is the position of the adatom about which the expansion in (3.13b) is performed.

### C. Logarithmic derivatives, $L_l(\epsilon)$

The required logarithmic derivatives are obtained from the numerical solution of (3.14) in which  $V(r)$  is the HF He potential. Writing  $R_l(r, \epsilon) \equiv u_l(r)/r$ , (3.14) reduces to the following in the region where  $v_m(z)$  is a constant:

$$-\frac{d^2}{dr^2}u_l(r) + \left( \frac{l(l+1)}{r^2} - \frac{4}{r} + 4 \int_0^\infty dr' r' R_{1s}^2(r') \frac{1}{r_{>}} + v_0 - \epsilon \right) u_l(r) - \frac{2}{2l+1} R_{1s}(r) \left( A_l r^{l+1} + r^{-l} \int_0^r dr' r'^{l+1} R_{1s}(r') u_l(r') - r^{l+1} \int_0^r dr' r'^{-l} R_{1s}(r') u_l(r') \right) = 0, \quad (3.41)$$

with

$$A_l = \int_0^\infty dr r^{-l} R_{1s}(r) u_l(r), \quad r_{>} = \max(r, r'). \quad (3.42)$$

$R_{1s}(r)$  is the He HF radial wave function. The numerical solution of (3.41) is discussed in Sec. IV.

### D. $a_{lm}(\epsilon\lambda)$

The fact that  $G_{lm, l'm'}$  and  $G'_{lm, l'm'}$  are diagonal in the approximation in which  $G^0(\vec{r}, \vec{r}', \epsilon)$  is replaced by  $G_d(\vec{r}, \vec{r}', \epsilon)$  simplifies (3.16) to an algebraic equation with the immediate solution

$$a_{lm}(\epsilon km) = \frac{\delta_{mm} b_{\vec{l}}(\epsilon km)}{\alpha r_0^2 j_l(i\alpha r_0) [i\alpha h_l^{(1)'}(i\alpha r_0) - L_l(\epsilon) h_l^{(1)}(i\alpha r_0)]}. \quad (3.43)$$

It is clear from this expression that  $a_{lm}(\epsilon km)$  reduces to  $\delta_{mm} b_{\vec{l}}(\epsilon km)$ , as it should, when the adatom potential is zero. It should be noted, however, that this solution fails if the bracketed quantity in the denominator vanishes. This happens if the adatom potential has a bound state at the energy  $\epsilon$ . This resonant condition implies that  $G^0(\vec{r}, \vec{r}', \epsilon)$  cannot be approximated by  $G_d(\vec{r}, \vec{r}', \epsilon)$  even in the large  $(z, z')$  region. The full Green's function as defined by (3.25) and (3.31) must be used and one must revert to Eq. (3.4) to obtain the change in density of states. For the helium adsorption problem this situation

does not arise and the approximations leading to (3.43) are justified.

To summarize the results of this section, we recall that  $\Delta\rho(\epsilon)$  is given by (3.6). For the choice of the unperturbed states in (3.36), the quantum numbers  $\lambda$  in (3.6) are  $m$  and  $k$  and the trace operation is explicitly

$$\text{Tr}_{(\lambda)} \rightarrow 2 \sum_{m=-\infty}^{\infty} \int_0^{\epsilon^{1/2}} dk, \quad (3.44)$$

where the factor of 2 accounts for the electronic spin. Using these results, (2.19) becomes

$$V_{\text{HF}}(Z) = \int_0^{\epsilon_F} d\epsilon \, 2 \sum_{m=-\infty}^{\infty} \int_0^{\epsilon^{1/2}} dk T_{km, km}(\epsilon), \quad (3.45)$$

with the  $T$  matrix given by (3.19). This is the basic result determining the metal-helium-atom repulsive interaction.

The asymptotic form of  $V_{\text{HF}}(Z)$  can be determined from (3.45) by noting that  $T_{km, km}(\epsilon)$  is proportional to  $e^{-2\beta Z}$ . In particular, if we define

$$\sum_{m=-\infty}^{\infty} T_{km, km}(\epsilon) \equiv \alpha_1^2(k) e^{-2\beta Z} t(k, \epsilon), \quad (3.46)$$

we find

$$V_{\text{HF}}(Z) \underset{Z \rightarrow +\infty}{\sim} (\Phi/k_F) \alpha_1^2(k_F) t(k_F, \epsilon_F) \frac{e^{-2(\Phi)1/2Z}}{Z^2}. \quad (3.47)$$

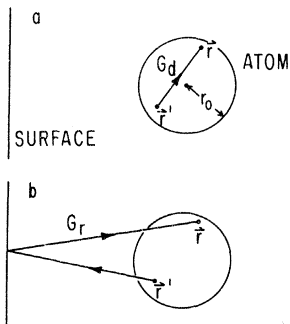


FIG. 2. Illustration of the two contributions of the metallic Green's function  $G^0(\vec{r}, \vec{r}', \epsilon)$  in the region of the atom.



The quantity  $t(k_F, \epsilon_F)$  is a property of the atomic potential and depends only on the position of the Fermi level relative to the vacuum zero. The remaining factor is proportional to the density in the asymptotic region.<sup>16</sup>

#### IV. APPLICATION TO HELIUM ADSORPTION

In this section we discuss the evaluation of (3.45) with  $T_{km, km}(\epsilon)$  given by (3.19). In calculating  $b_i(\epsilon km)$  and  $b'_i(\epsilon km)$  from (3.40) we require  $u_k(z)$  in the form  $a_1(k)e^{-\beta z}$ . The asymptotic amplitude  $a_1(k)$  is determined by the details of the free metal surface. In our calculations we have used the Lang-Kohn (LK)<sup>10</sup> self-consistent potentials for the jellium model to determine  $a_1(k)$  subject to certain modifications. The LK potentials, which are given for integral values of  $r_s$ , were scaled such that the potential barrier had unit amplitude. The potential for an arbitrary value of  $r_s$  was then obtained by linearly interpolating between the LK results. Since the scaled LK potentials varied smoothly as a function of  $r_s$ , this interpolation should be reliable. Finally, this interpolated potential was rescaled such that the effective barrier height,  $v_0$ , had a magnitude equal to  $(k_F^2 + \Phi)$ , where  $\Phi$  is the (experimental) work function. By using the experimental work function we have attempted to reproduce the correct asymptotic density. The amplitude  $a_1(k)$  was then obtained by numerically solving (3.28). In the region of the equilibrium position of the He atom, the asymptotic form  $a_1(k)e^{-\beta z}$  was found to be a good approximation to the wave function  $u_k(z)$ .

The logarithmic derivatives,  $L_l(\epsilon)$ , used in our calculations were obtained by numerically solving the HF equation (3.41). The atomic He wave function was taken to be

TABLE I. Hartree-Fock logarithmic derivatives as a function of the energy (relative to the vacuum level) for  $l=0, 1$ , and 2 at a radius  $r_0=4.5$  a.u.

$-\epsilon$ (eV)	$L_0$	$L_1$	$L_2$
0	0.1090	0.2136	0.4435
2	0.2487	0.3390	0.5341
4	0.3677	0.4474	0.6174
6	0.4722	0.5435	0.6948
8	0.5659	0.6304	0.7672
10	0.6512	0.7102	0.8355
12	0.7300	0.7842	0.9001
14	0.8035	0.8534	0.9616
16	0.8728	0.9188	1.0204
18	0.9386	0.9807	1.0767
20	1.0022	1.0397	1.1309

$$R_{1s}(r) = 2.95256 e^{-1.453r} + 1.79914 e^{-2.906r}. \quad (4.1)$$

This form was chosen since it had previously been used<sup>17</sup> to define zero-energy  $e^-$ -He pseudopotentials and it was of interest to compare the results based on the HF and pseudopotential logarithmic derivatives. The pseudopotential in the HF approximation is discussed in an appendix.

The infinite range integrals in (3.41) were truncated at  $r=5$  a.u. and the resulting equation was then solved iteratively. The logarithmic derivatives computed from this solution at  $r=4.5$  a.u. are given in Table I as a function of the energy. The truncation at  $r=5$  a.u. introduced a negligible error; the variation of the logarithmic derivative between  $r=4.5$  and  $r=5$  a.u. in fact corresponded to the zero-potential behavior.

Using the above results,  $V_{HF}(Z)$  was calculated as a function of  $Z$  for the simple and noble metals listed in Table II. It was found to be sufficient to

TABLE II. Characteristic properties of He adsorbed on various metals. The energies are given in both meV and degrees Kelvin.

Metal	$r_s$	$\Phi^a$ (eV)	$C^b$ (eV Å <sup>3</sup> )	$Z_0^b$ (Å)	$-E_0$ (meV) (K)		Zero-point energy (meV) (K)		$\langle Z \rangle_0$ (Å)		$\Delta E_{10}$ (meV) (K)	
					<sup>3</sup> He	<sup>4</sup> He	<sup>3</sup> He	<sup>4</sup> He	<sup>3</sup> He	<sup>4</sup> He	<sup>3</sup> He	<sup>4</sup> He
Al	2.07	4.19	0.202	0.544	3.44(40.0)	3.65(42.4)	1.76(20.4)	1.55(18.0)	3.79	3.73	2.16(25.0)	2.05(23.8)
Mg	2.65	3.66	0.153	0.478	1.65(19.1)	1.78(20.6)	1.12(13.0)	0.99(11.5)	4.27	4.18	1.19(13.8)	1.17(13.5)
Li	3.28	3.1	0.117	0.428	0.77( 8.9)	0.85( 9.8)	0.70( 8.1)	0.62( 7.2)	4.91	4.77	0.63( 7.3)	0.64( 7.4)
Na	3.99	2.7	0.092	0.388	0.41( 4.7)	0.46( 5.3)	0.49( 5.7)	0.44( 5.1)	5.51	5.31	0.36( 4.2)	0.38( 4.4)
K	4.96	2.39	0.070	0.356	0.20( 2.4)	0.24( 2.7)	0.34( 4.0)	0.30( 3.5)	6.23	5.95	0.19( 2.2)	0.21( 2.5)
Rb	5.23	2.21	0.065	0.351	0.15( 1.8)	0.18( 2.1)	0.28( 3.3)	0.25( 2.9)	6.64	6.30	0.15( 1.7)	0.17( 1.9)
Cs	5.63	2.14	0.058	0.345	0.13( 1.5)	0.15( 1.8)	0.25( 2.8)	0.23( 2.6)	6.84	6.47	0.12( 1.4)	0.14( 1.6)
Cu	2.67	4.65	0.225	0.220	3.34(38.8)	3.55(41.2)	1.74(20.2)	1.53(17.8)	3.66	3.59	2.08(24.2)	1.98(23.0)
Ag	3.02	4.0	0.249	0.196	3.34(38.7)	3.53(41.0)	1.61(18.7)	1.42(16.5)	3.73	3.67	2.01(23.4)	1.90(22.1)
Au	3.01	5.22	0.274	0.155	5.61(65.1)	5.91(68.6)	2.39(27.7)	2.09(24.3)	3.23	3.17	3.13(36.3)	2.92(34.0)

<sup>a</sup> From Ref. 27.

<sup>b</sup> From Ref. 5.

include only the terms up to  $|m|=2$  in the summation over  $m$ . The  $m=0$  term is positive, giving a repulsive contribution. By contrast, the  $m \neq 0$  terms are negative; their contribution was typically 25% of the  $m=0$  term in magnitude. Thus, they represent an important attractive component. This result indicates that the use of a  $\delta$ -function pseudopotential whose strength is determined by the zero-energy  $s$ -wave  $e^-$ -He scattering length is inadequate in estimating the repulsion. The rapidly varying metallic density at the surface means that higher  $l$  components in the wavefunction expansion (3.13b) are appreciable. These components feel a strong attractive potential.

The calculations were also repeated using a limiting radius of  $r_0=5$  a.u. The results differed negligibly from the  $r_0=4.5$  a.u. case, demonstrating their independence of  $r_0$  for  $r_0 > 4.5$  a.u.

The total He-metal potentials, as calculated from (2.3) with  $V_{\text{corr}}(Z)$  given by (2.4), are shown in Figs. 3 and 4. For the simple metals, the potential systematically weakens as the density is decreased and the minimum moves out to larger values of  $Z$ . This behavior is essentially due to the decreasing strength of the Van der Waals interaction as determined by the values of  $C$  and  $Z_0$ . Although one would similarly expect the repulsive energy to decrease with density, this trend is compensated by the decreasing work function.<sup>16</sup> The net effect is that the repulsive potential  $V_{\text{HF}}(Z)$  is rather insensitive to the mean metallic density. For example, at  $Z=3.0$  Å, the value of  $V_{\text{HF}}(Z)$  decreases by only 30% as the density is varied between  $r_s=2.07$  and  $r_s=5.63$ . This cancellation of the effects of the decreasing density and the decreasing work function makes the Van der Waals energy the determining factor in the variation of the total potential.

These trends for the simple metals are opposite to those found by Kleiman and Landman.<sup>7</sup> These authors used metallic densities which did not correspond to the observed work functions and therefore underestimated the amplitude of the density in the asymptotic region for the less dense metals. In addition, the variation of  $Z_0$  with  $r_s$  is an important factor in determining the Van der Waals potential. Our values for  $V_{\text{corr}}(Z)$  correctly include the effects of the reference plane position and therefore yield stronger attractive potentials. The combined effects of the incorrect asymptotic densities and the incorrect reference plane position accounts for the different trends.<sup>28</sup>

Our results for the noble metals do not follow the trends for the simple metals since the Van der Waals interaction does not scale with the valence electron density in the same way. The oscillator strengths for the core electron transi-

tions<sup>18</sup> make a significant contribution to  $C$ .<sup>5</sup> As can be seen in Fig. 4, the potentials for Cu and Ag are very similar. Although their bulk densities are quite different, their Van der Waals coefficients are nearly equal. In addition the relative magnitude of the work functions compensates for the density difference in the determination of  $V_{\text{HF}}(Z)$ . On the other hand, Au has both a larger work function and a larger value of  $C$ ; these factors contribute to the deeper potential well for this metal.

Previously, a local pseudopotential was successfully used to account for low-energy  $e^-$ -He scattering.<sup>17</sup> Because of the computational ease in using a local potential as compared to the HF solution, it was of interest to repeat the above calculations using the local potential derived in the appendix. These calculations were performed for the case of Al and the resulting He-Al potential is shown as the dashed curve in Fig. 3. The magnitude of the repulsive energy is only slightly larger relative to the HF result. It therefore appears that the local pseudopotential provides a good representation of the  $e^-$ -He potential even for those states which have a significant spatial variation on the scale of the atom itself.

Since the mass of the He atom is small, it is necessary to take its zero-point energy into account when determining the binding energy. Using the potentials in Figs. 3 and 4, the Schrödinger equation for the He wave function was solved numerically and the results are listed in Table II. Values for the binding energy  $-E_0$ , zero-point energy, the first excitation energy  $\Delta E_{10}=E_1-E_0$ , and the mean position  $\langle Z \rangle_0$  are given for both isotopes of He. The binding energy decreases monotonically with decreasing density for the simple metals, varying, in the case of <sup>4</sup>He, from 42.4 to 1.8 K on going from Al to Cs. The corresponding mean positions vary from 3.7 to 6.5 Å relative to the jellium background. The atom is very weakly bound to all the alkali metals and quite generally, its equilibrium position is far from the metal surface. These results are summarized in Fig. 5 for the case of <sup>4</sup>He. As can be seen, the equilibrium position varies linearly with  $r_s$  whereas the binding energy behaves approximately as  $r_s^{-3}$ , i.e., proportional to the density. The binding energy of <sup>3</sup>He is typically 10% less than that of <sup>4</sup>He.

In the case of the noble metals, the binding energy for both Cu and Ag is about 40 K and for Au it is 69 K. It is of interest to note that recent measurements<sup>19,20</sup> of the binding energy of Xe on Cu and Ag suggest that the potentials for these metals are indeed similar. This is consistent with our results for He, although one cannot justify, at the present time, the similarity of the po-

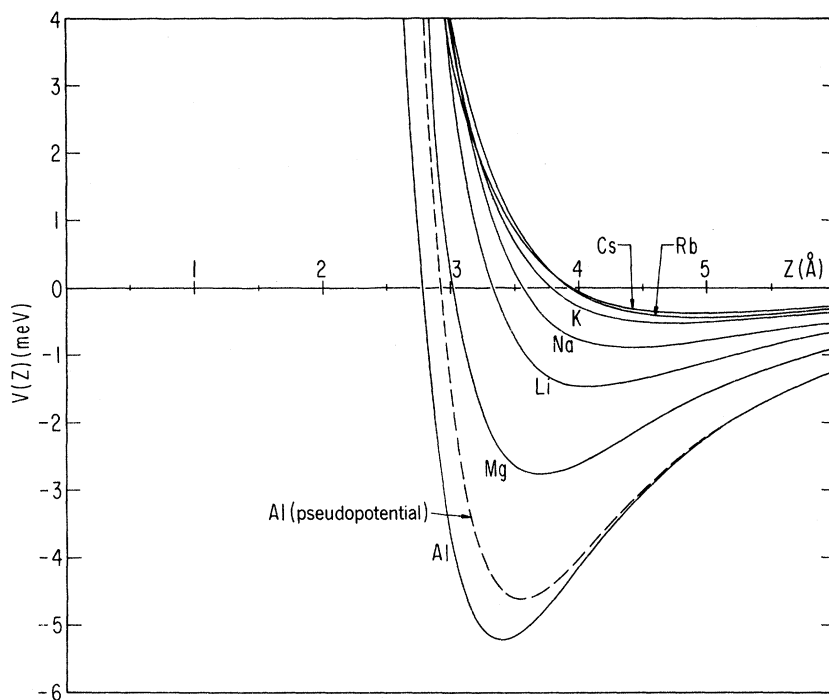


FIG. 3. He-metal potentials for various simple metals. The solid lines are the results using the Hartree-Fock potential [see Eq. (3.41)] and the dashed curve is based on the pseudopotential given in the Appendix. The origin is chosen at the edge of the jellium background.

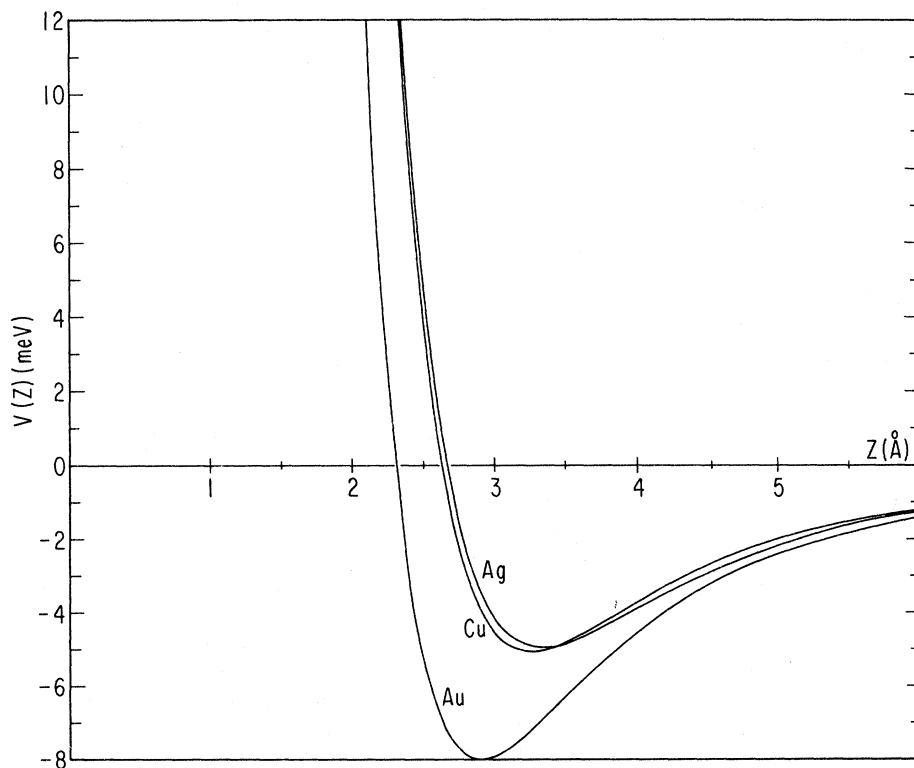


FIG. 4. Physisorption potentials for He on the noble metals.

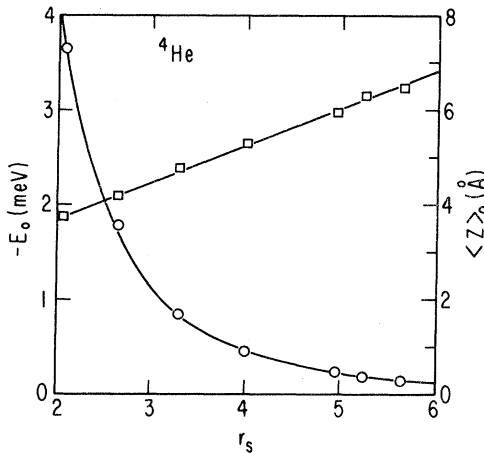


FIG. 5. Binding energy (○) and equilibrium position (□) as a function of  $r_s$  for  ${}^4\text{He}$  on the metals shown in Fig. 3.

tentials for these two metals, for each of the rare-gas atoms. Indeed, it should be pointed out that other measurements<sup>21</sup> of the Xe-Ag binding energy do not support this conclusion.

Although the adsorption of He on solid surfaces has been studied extensively, values for the binding energy of monolayer He films on metal surfaces do not seem to be available. The binding of He on argon-plated copper<sup>22</sup> appears similar to our value for the bare surface. Furthermore, the binding energy on graphite<sup>23</sup> is of the same order of magnitude. However, similar measurements for bare metal surfaces are required to decide whether our theory is quantitatively reliable.

In Fig. 6 we have plotted the electronic density corresponding to the state  $\psi_{\epsilon_F, k_F, 0}^{(+)}(\vec{r})$  in a direction perpendicular to the surface and through the center of the atom. This density is in fact similar to the total metallic density, since far from the surface, only those states with energies  $\epsilon$  close to  $\epsilon_F$  and wave vectors  $k$  close to  $k_F$  contribute significantly. As can be seen, there is a large pile-up of charge in the vicinity of the He atom and a depletion of charge in the region between the adatom and the surface itself. The difference in the charge densities with and without the atom is localized in the atomic region decaying slowly in the direction of the metal. However, the difference far from the atom is small and, as stated previously, of the order of the overlap.

The redistribution of charge indicated in Fig. 6 gives rise to a dipole moment which points away from the surface. Such a dipole moment has the effect of increasing the work function and is opposite in sense to that observed for Xe on metallic surfaces.<sup>19</sup> However, it should be noted that there

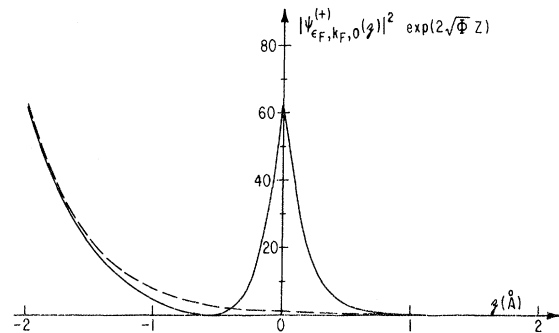


FIG. 6. Charge density of the metallic electrons in the vicinity of the helium atom. The dashed curve is the unperturbed metallic density.

is an independent contribution to the dipole moment which arises from the Van der Waals interaction itself.<sup>24,25</sup> This latter contribution decreases the work function; in the case of He it is probably small because of the small atomic polarizability. Thus, the moment we have calculated, which is related to the charge overlap, might well dominate. A quantitative estimate of the dipole moment associated with the He atom would, however, require determining the fully self-consistent density and goes beyond the calculation of this paper.

#### APPENDIX

The total atomic potential in (2.15) is given by

$$(\hat{V}\psi)(\vec{r}) \equiv \left( -\frac{4}{r} + 4 \int d\vec{r}' \frac{|\psi_a^0(\vec{r}')|^2}{|\vec{r} - \vec{r}'|} \right) \psi(\vec{r}) - 2 \int d\vec{r}' \frac{\psi_a^0(\vec{r}')^* \psi(\vec{r}')}{|\vec{r} - \vec{r}'|} \psi_a^0(\vec{r}). \quad (\text{A1})$$

Following Kestner *et al.*,<sup>17</sup> we introduce a pseudopotential

$$\hat{V}_{ps} = \hat{V} + \hat{V}_R \quad (\text{A2})$$

where  $\hat{V}_R$  is the nonlocal repulsive potential defined by

$$(\hat{V}_R\varphi)(\vec{r}) \equiv - \int d\vec{r}' \psi_a^0(\vec{r}')^* (\hat{V}\varphi)(\vec{r}') \psi_a^0(\vec{r}). \quad (\text{A3})$$

An approximate local potential for each angular momentum component  $l$  can be obtained from the above as follows. Writing

$$\varphi(\vec{r}) = R_l(r) Y_{lm}(\Omega) \quad (\text{A4})$$

the radial (pseudo) wave function  $R_l(r)$  behaves as  $r^l$  for small  $r$ . Assuming that this functional form represents the main spatial dependence in the atomic region, the exchange part of the potential in (A1) becomes

$$\hat{V}_x^{(l)} \varphi \equiv -2 \int d\vec{r}' \frac{\psi_a^0(\vec{r}')^* \varphi(\vec{r}')}{|\vec{r} - \vec{r}'|} \psi_a^0(\vec{r}) \approx -\frac{8\pi}{2l+1} \left( \int_0^r dr' \frac{r'^{2(l+1)}}{r^{2l+1}} \psi_a^0(r') + \int_r^\infty dr' r' \psi_a^0(r') \right) \psi_a^0(r) \varphi(r). \quad (\text{A5})$$

Using the atomic He wave function given in (4.1), (A1), (A3), and (A5) yield the local potential<sup>26</sup>

$$V^{(l)}(r) = -2.84185 e^{-2\Lambda r}/r - 1.02618 e^{-3\Lambda r}/r - 0.13190 e^{-4\Lambda r}/r \\ - 4.12921 e^{-2\Lambda r} - 2.23656 e^{-3\Lambda r} - 0.38330 e^{-4\Lambda r} + V_x^{(l)}(r) + \delta_{l,0} V_R(r), \quad (\text{A6})$$

where

$$V_x^{(l)} = - \left[ 9.91523 \left( \frac{2(l+1)}{(\Lambda r)^{2l+1}} I_{2l}(\Lambda r) + I_0(\Lambda r) - 1 \right) + 1.51046 \left( \frac{2(l+1)}{(2\Lambda r)^{2l+1}} I_{2l}(2\Lambda r) + I_0(2\Lambda r) - 1 \right) \right] \psi_a^0(r) \quad (\text{A7})$$

and

$$V_R(r) = 11.27970 e^{-\Lambda r} + 6.87327 e^{-2\Lambda r}. \quad (\text{A8})$$

In (A7), we have defined

$$I_n(t) = \int_0^t ds s^n e^{-s}, \quad (\text{A9})$$

and  $\Lambda = 1.453$ .

As a check on the potential in (A6), the  $l=0, 1, 2$  phase shifts were calculated at  $k=0.5$  a.u. The results, compared with the HF values, were  $\delta_0 = -0.59$  ( $\delta_0^{\text{HF}} - \pi = -0.71$ ),  $\delta_1 = 0.043$  ( $\delta_1^{\text{HF}} = 0.042$ ),  $\delta_2 = 0.00083$  ( $\delta_2^{\text{HF}} = 0.00084$ ). As can be seen, the local potential in (A5) is a good representation of the nonlocal HF exchange for  $l=1, 2$  in this energy range.

\*Supported in part by the Office of Naval Research and the National Science Foundation.

†Present address: Department of Physics, Queen's University, Kingston, Ontario, Canada K7L 3N6.

<sup>1</sup>D. M. Young and A. D. Crowell, *Physical Adsorption of Gases* (Butterworths, Washington, 1962).

<sup>2</sup>H. Margenau and N. R. Kestner, *Theory of Intermolecular Forces* (Pergamon, Oxford, 1969); J. D. Hirschfelder and W. J. Meath, *Adv. Chem. Phys.* **12**, 3 (1967).

<sup>3</sup>E. M. Lifshitz, *Zh. Eksp. Teor. Fiz.* **29**, 94 (1955) [*Sov. Phys.-JETP* **2**, 73 (1956)].

<sup>4</sup>C. Mavroyannis, *Mol. Phys.* **6**, 593 (1963).

<sup>5</sup>E. Zaremba and W. Kohn, *Phys. Rev. B* **13**, 2270 (1976).

<sup>6</sup>P. I. Cohen, J. Unguris, and M. B. Webb (unpublished).

<sup>7</sup>G. G. Kleiman and U. Landman, *Phys. Rev. B* **8**, 5484 (1973).

<sup>8</sup>"Metallic" refers to those states which extend into the metal and overlap the adatom.

<sup>9</sup>R. G. Gordon and Y. S. Kim, *J. Chem. Phys.* **56**, 3122 (1972); Y. S. Kim and R. G. Gordon, *J. Chem. Phys.* **61**, 1 (1974).

<sup>10</sup>N. D. Lang and W. Kohn, *Phys. Rev. B* **1**, 4555 (1970).

<sup>11</sup>J. S. Langer and V. Ambegaokar, *Phys. Rev.* **121**, 1090 (1961).

<sup>12</sup>R. Dashen, S. Ma, and H. J. Bernstein, *Phys. Rev.* **187**, 345 (1969).

<sup>13</sup>See, for example, J. R. Taylor, *Scattering Theory* (Wiley, New York, 1972), Chap. 10.

<sup>14</sup>P. M. Morse and H. Feshbach, *Methods of Theoretical*

*Physics* (McGraw-Hill, New York, 1953), Chap. 7.

<sup>15</sup>M. Abramowitz and I. A. Stegun, *Handbook of Mathematical Functions* (Dover, New York, 1972).

<sup>16</sup>The density in the region  $z \rightarrow +\infty$  is given by  $n(z) \approx (\Phi/\pi^2 k_F) \alpha_1^2(k_F) \exp[-2(\Phi)^{1/2} z]/z^2$ .

<sup>17</sup>N. R. Kestner, J. Jortner, M. H. Cohen, and S. A. Rice, *Phys. Rev.* **140**, A56 (1965).

<sup>18</sup>J. J. Rehr, E. Zaremba, and W. Kohn, *Phys. Rev. B* **12**, 2062 (1975).

<sup>19</sup>B. E. Nieuwenhuys, O. G. Van Aardenne, and W. M. H. Sachtler, *Chem. Phys.* **5**, 418 (1974).

<sup>20</sup>G. McElhiney, H. Papp, and J. Pritchard, *Surf. Sci.* **54**, 617 (1976).

<sup>21</sup>P. I. Cohen, J. Unguris, and M. B. Webb, *Bull. Am. Phys. Soc.* **20**, 406 (1975).

<sup>22</sup>J. G. Dash, R. E. Peierls, and G. A. Stewart, *Phys. Rev. A* **2**, 932 (1970).

<sup>23</sup>G. J. Goellner, J. G. Daunt, and E. Lerner, *J. Low Temp. Phys.* **21**, 347 (1975).

<sup>24</sup>P. R. Antoniewicz, *Phys. Rev. Lett.* **32**, 1424 (1974).

<sup>25</sup>E. Zaremba, *Phys. Lett. A* **57**, 156 (1976).

<sup>26</sup>The coefficient of  $e^{-2\Lambda r}$  in Eq. (16) of Ref. 17 should read 2.06461 rather than 2.206461.

<sup>27</sup>N. D. Lang and W. Kohn, *Phys. Rev. B* **3**, 1215 (1971).

<sup>28</sup>The inclusion of spatial dispersion in G. G. Kleiman and U. Landman, *Phys. Rev. Lett.* **33**, 524 (1974), yields a dependence of the binding energy on the metallic density similar to that obtained in this paper.